

LA-UR-95-3332

Title:

SOLIDIFICATION BEHAVIOR DURING DIRECTED LIGHT FABRICATION

**DISCLAIMER**

This report was prepared as an account of work sponsored by an agency of the United States Government. Neither the United States Government nor any agency thereof, nor any of their employees, makes any warranty, express or implied, or assumes any legal liability or responsibility for the accuracy, completeness, or usefulness of any information, apparatus, product, or process disclosed, or represents that its use would not infringe privately owned rights. Reference herein to any specific commercial product, process, or service by trade name, trademark, manufacturer, or otherwise does not necessarily constitute or imply its endorsement, recommendation, or favoring by the United States Government or any agency thereof. The views and opinions of authors expressed herein do not necessarily state or reflect those of the United States Government or any agency thereof.

Author(s):

DAN J. THOMA, MST-6  
GARY K. LEWIS, MST-6  
RON B. NEMEC, MST-6

Submitted to:

ASM BOOK "BEAM PROCESSING OF ADVANCED MATERIALS"

DISTRIBUTION OF THIS DOCUMENT IS UNLIMITED

**MASTER**

xy



# Los Alamos

NATIONAL LABORATORY

Los Alamos National Laboratory, an affirmative action/equal opportunity employer, is operated by the University of California for the U.S. Department of Energy under contract W-7405-ENG-36. By acceptance of this article, the publisher recognizes that the U.S. Government retains a nonexclusive, royalty-free license to publish or reproduce the published form of this contribution, or to allow others to do so, for U.S. Government purposes. The Los Alamos National Laboratory requests that the publisher identify this article as work performed under the auspices of the U.S. Department of Energy.

## **DISCLAIMER**

**Portions of this document may be illegible  
in electronic image products. Images are  
produced from the best available original  
document.**

# SOLIDIFICATION BEHAVIOR DURING DIRECTED LIGHT FABRICATION

D.J. Thoma, G.K. Lewis, and R.B. Nemec

Los Alamos National Laboratory, Materials Science and Technology Division,  
Mail Stop G770, Los Alamos, NM 87545 USA

## Abstract

Directed light fabrication (DLF) is a process that fuses gas delivered metal powders within a focal zone of a laser beam to produce fully dense, 3-dimensional metal components. A variety of materials have been processed with DLF, ranging from steels to tungsten, and including intermetallics such as NiAl and MoSi<sub>2</sub>. To evaluate the processing parameters and resulting microstructures, solidification studies have been performed on defined alloy systems. For example, solidification cooling rates have been determined based upon secondary dendrite arm spacings in Fe-based alloys. In addition, eutectic spacings have been used to define growth velocities during solidification. Cooling rates vary from  $10^1$ - $10^5$  K s<sup>-1</sup> and growth rates vary between 1-50 mm s<sup>-1</sup>. As a result, process definition has been developed based upon the microstructural development during solidification.

DIRECTED LIGHT FABRICATION (DLF) is a rapid prototyping process that fuses gas delivered metal powders within a focal zone of a laser beam to produce 3-dimensional metal components [1]. The focal zone of the laser beam is programmed to move along or across a part cross-section, and coupled with a multi-axis sample stage, complex metal geometries can be produced. The DLF technique offers unique advantages over conventional thermomechanical processes in that many labor and equipment intensive steps can be avoided. For example, typical processing of metals into desired shapes and assemblies involves casting and metal forming (rolling, stamping, forging, extrusion) followed by machining and joining operations. The DLF process yields a final geometry from a single piece of equipment and the appropriate software control.

Development of the plastics rapid prototyping processes since the early 1980's demonstrates the feasibility of producing parts from three dimensional solid model

designs by a single process and a single piece of equipment [2]. The processing of parts are made by additive deposition of planar layers of plastic material until the complete part is formed. However, this processing has been restricted primarily to plastics and not successfully extended to produce fully dense metal parts. Potential metal rapid prototyping processes include liquid metal spraying, plasma spraying, electron beam vapor deposition, and investment casting processes. These metal processing techniques are non-directional deposition processes that require mold patterns or masks to gain the detail for complex parts and assemblies.

Since DLF processing offers unique capabilities and advantages for rapid prototyping of complex metal components, an examination of the microstructural development is required to define and optimize the processed materials. The intent of this study is to address the solidification behavior during DLF processing of simple geometries to characterize the technique.

## Experimental Procedure

The DLF process consists of generating tool paths from computer generated 3-dimensional solid models. The tool paths continuously move the focal zone of the laser systematically along areas of the part to fuse metal powder particles that are gas delivered to the focal zone. A schematic diagram of the process is shown in Figure 1. Three Nd-YAG pulsed lasers (1 KW) that are connected in series to simulate a continuous wave (CW) laser are delivered via fiber optics to a sealed boom that holds the laser focusing head and is attached to the "z" (vertical) axis. The focused laser beam enters the chamber through a quartz window in a nozzle that also delivers the metal powder to the focal zone. The entire process takes place in an inert gas box connected to a dry train that reduces the oxygen content to 5 ppm or less. In the upper right of the schematic diagram is a chamber that can be evacuated and back-filled with an inert gas that contains the powder feeder. The powder feeder entrains the powder in an

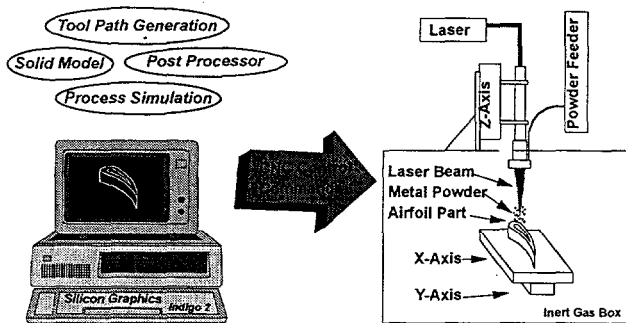


Figure 1 - Schematic diagram of the DLF process

argon stream that delivers the powder to the laser focus nozzle and then to the focal zone. A positioning controller drives the "x", "y", and "z" tables, switches the laser shutter and powder feeder on and off, and controls various gas flows.

The deposition process is started on a metal plate that is cut off after deposition is complete. Typically, the laser beam is rastered onto the base plate before powder feeding starts. The preheated base plate promotes better adhesion (and therefore better heat transport) for the initial deposited powder. Powders are then fed into the focal zone and the part is deposited in a continuous fashion.

For the purpose of evaluating the solidification behavior in DLF, one dimensional and two-dimensional experimental studies were conducted. The one dimensional studies consisted of only z-direction growth of rods (~40 mm long and 3 mm in diameter). Plates (or walls) were produced for the two dimensional study by building up horizontal layers of continuously fused powder. The walls typically have dimensions of 25 mm x 40 mm x 3 mm (length x height x width). The materials explored were Ag-19wt%Cu, Fe-24.8wt.%Ni, 316 stainless steel, Al-33wt%Cu, W, MoSi<sub>2</sub>, and NiAl. All starting powders were approximately 50  $\mu\text{m}$  in diameter and are commercially available.

## Results

**Materials.** A variety of metals and alloys have been processed with the DLF technique. Examples of the range of materials are demonstrated in Figure 2, where the starting powder, typical rods, cross-sections of the rods, and the fracture surfaces of hand-broken rods are illustrated. The samples of 316 stainless steel, tungsten, NiAl, and MoSi<sub>2</sub> are all fully dense, as-solidified product. The intermetallics display a brittle fracture surface which is typical for these materials, and the stainless steel was ductile. The pure tungsten could be bent to a right angle, but once bent back, a brittle failure occurred.

**Solid/Liquid Interface.** A longitudinal cross-section of a Ag-19%Cu rod processed by DLF is shown in Figures 3a. The rod has continuous dendrites along the length of the sample. Since the microstructural development in the DLF processed sample displays continuous morphologies, a constant solid/liquid interface must be

maintained. A schematic diagram of the rod growth process is shown in Figure 3b. Apparently, a molten layer of the alloy resides at the top of the rod, and the solid dendrites continuously grow (in the mushy zone) during the process. Of course, if the molten zone is too large or too small, the stability and integrity of the process decreases. Therefore, the processing variables such as laser power, beam speed, and powder feed rate are critical in producing uniform samples.

Longitudinal cross-sections of a 316 stainless steel plate sample are shown in Figures 4a and 4b, and a schematic diagram of the plate growth is shown in Figure 4c. As with the rod, the dendritic structure is continuous in the sample. Strong evidence of epitaxial growth off of the prior solid interface can be observed with each beam pass, and the zig-zag growth orientation of the layers results from the alternate processing directions of the multiple laser beam passes. In addition, a thin heat affected zone (~2  $\mu\text{m}$ ) is evident with each beam pass. In the schematic drawing of the plate growth, the mushy zone exists continuously, even at the corners of the plate, to maintain a constant solid/liquid interface. The continuous microstructural development in the plate growth supports the existence of the continuous solid/liquid interface during processing.

**Cooling Rates.** Secondary arm spacing analysis is a common technique to experimentally evaluate cooling rates during solidification [3]. Indeed, both empirical and theoretical studies have shown that the secondary dendrite arm spacing,  $\lambda_2$ , is related to the local solidification time,  $t_f$ , by the relation

$$\lambda_2 = At_f^n \quad (1)$$

where  $A$  is a constant and  $n \approx 1/3$  [3]. Alternatively, the local solidification time can be expressed as

$$t_f = \frac{\Delta T_s}{GV} \quad (2)$$

where  $\Delta T_s$  is the temperature range of solidification (K),  $G$  is the thermal gradient at the solid/liquid interface (K/m), and  $V$  is the solidification velocity (m/s). The cooling rate,  $\varepsilon$ , can be expressed as the product of  $G$  and  $V$ . As a result, Eq. (1) can be modified to a direct form relating the secondary dendrite arm spacing to cooling rate as,

$$\lambda_2 = B\varepsilon^{-n} \quad (3)$$

where  $B = A(\Delta T_s)^n$ .

Empirical relationships relating the cooling rate to the secondary dendrite arm spacing have been well-documented for Fe-25wt.%Ni [4] and 316 stainless steel [5,6]. For Fe-25wt.%Ni, the relationship is

$$\lambda_2 = 60\varepsilon^{-0.32} \quad (4)$$

The cooling rate has the units of (K/s) and  $\lambda_2$  is expressed in microns. For 316 stainless steel, the empirical relationship is

$$\lambda_2 = 25\varepsilon^{-0.28} \quad (5)$$

Both rods and plates of the two Fe-based alloys were grown by the DLF process, and example microstructures are shown in Figures 5a and 5b, respectively. The secondary

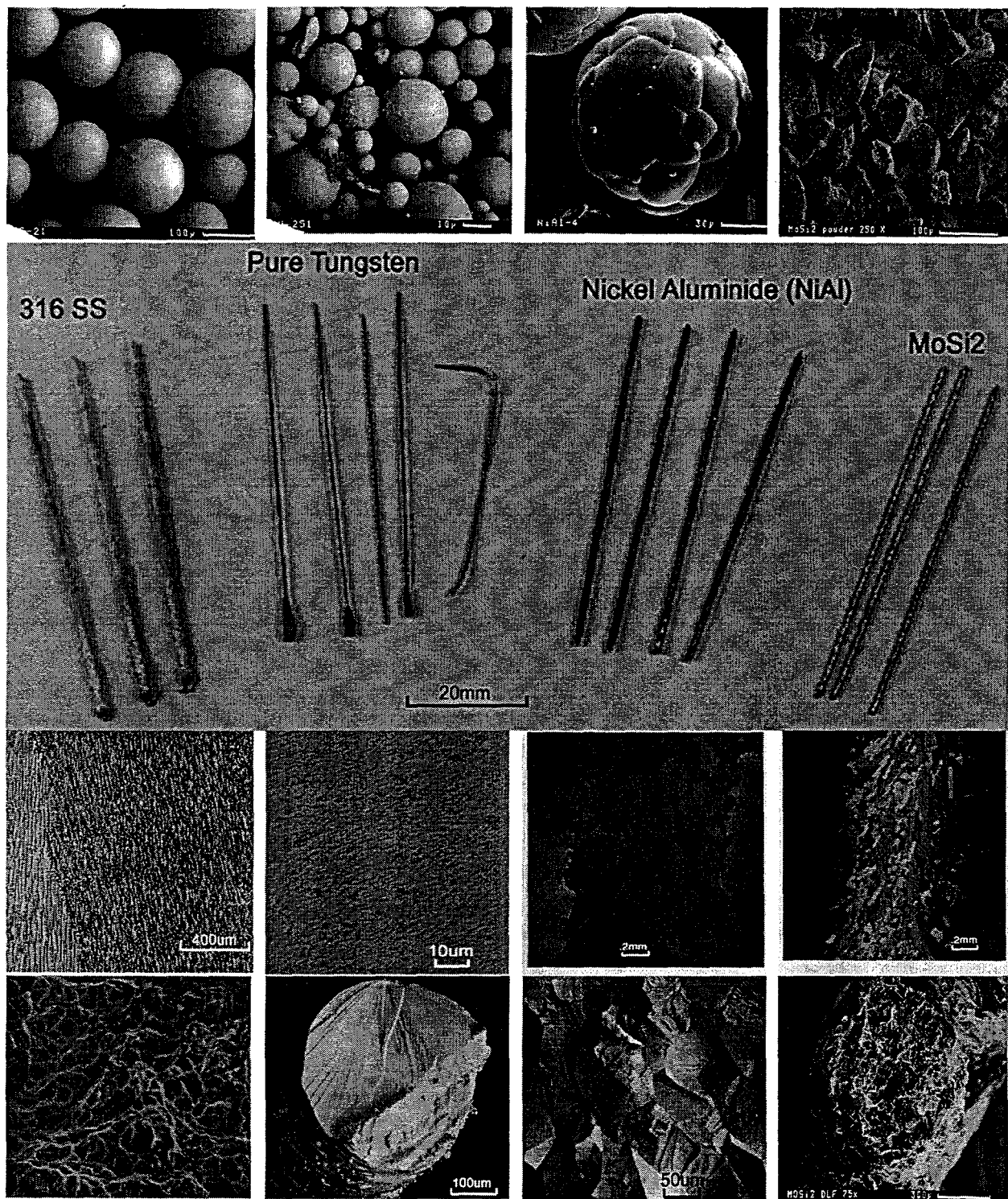
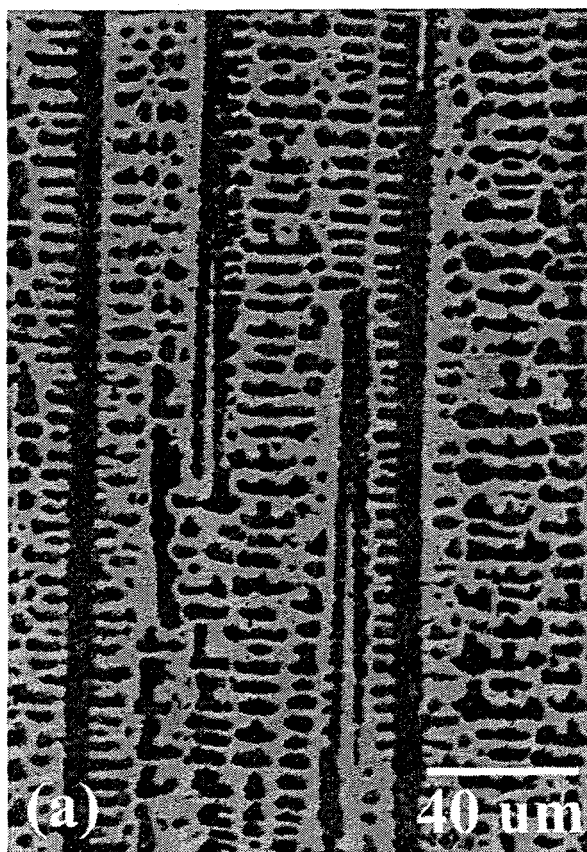
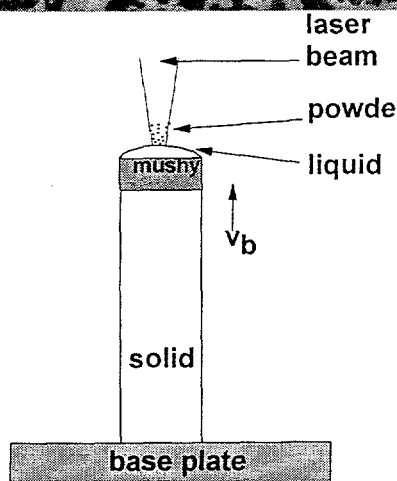


Figure 2 - Starting powders, rods, cross-section microstructures, and fracture surfaces of rods for 316 stainless steel, tungsten, NiAl, and MoSi<sub>2</sub>.



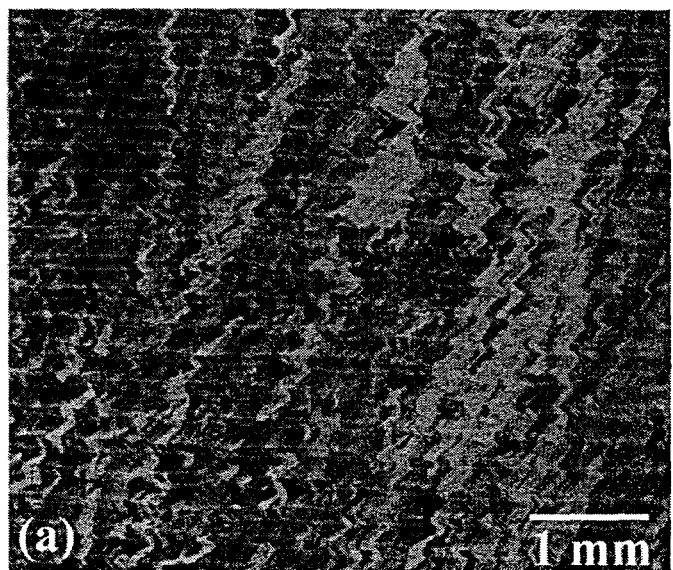
(a)

40  $\mu\text{m}$



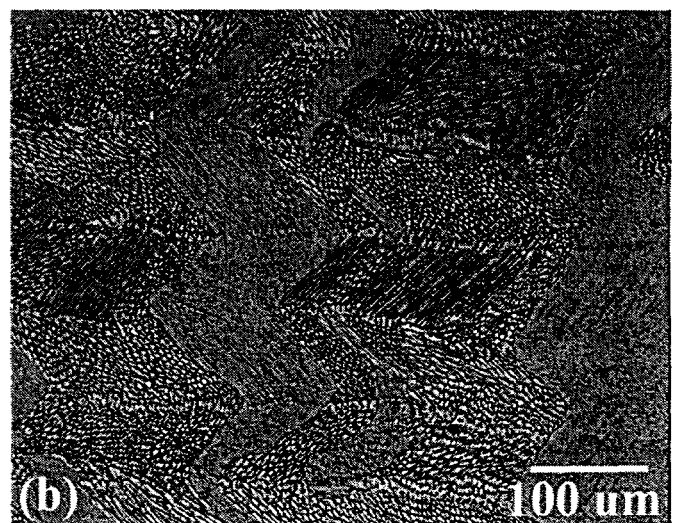
(b)

Figure 3 - (a) Cross-section micrograph of Ag-19wt.%Cu showing continuous dendrites, and (b) a schematic diagram of the processing of a rod



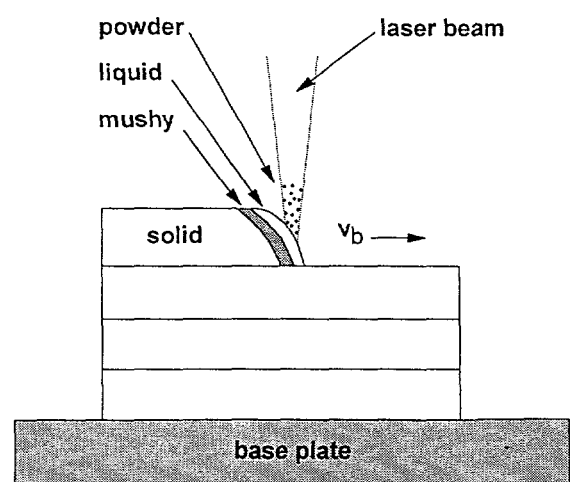
(a)

1 mm



(b)

100  $\mu\text{m}$



(c)

Figure 4 - (a) Low magnification and (b) high magnification cross-sections of a 316 stainless steel wall, and (c) a schematic diagram of the wall growth.

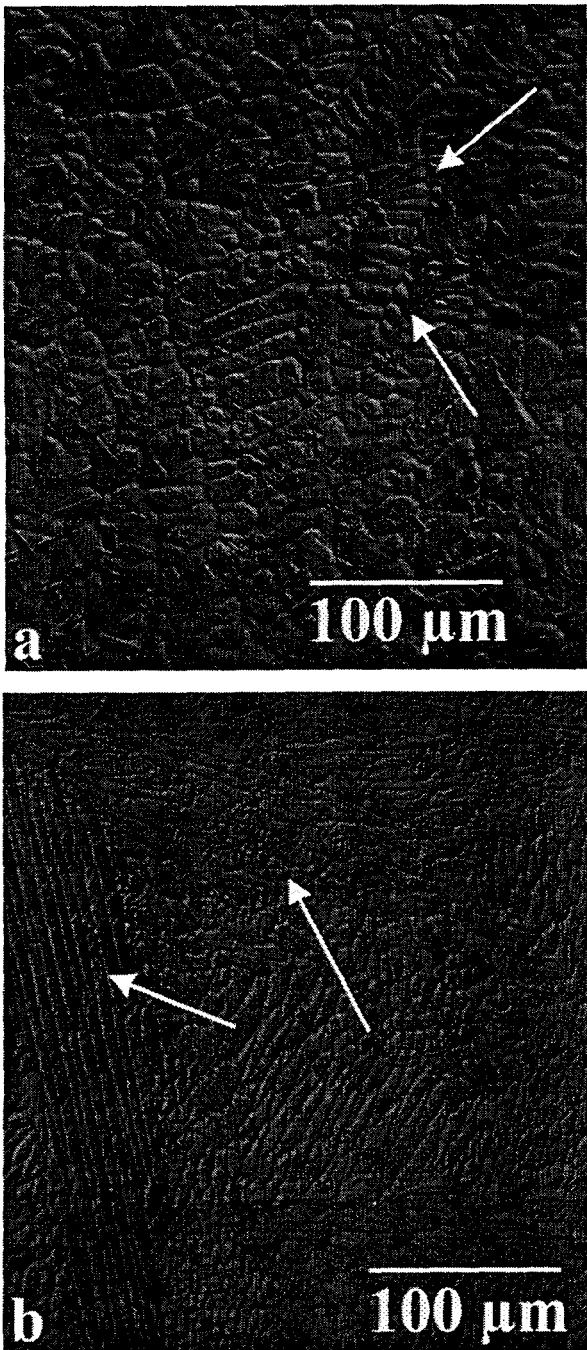


Figure 5 - Cross-section micrographs of an Fe-25wt.%Ni (a) rod, and (b) plate. Arrows indicate secondary dendrite arms

arms spacings are indicated on the micrographs. For these two particular cases, secondary dendrite arm spacing in the rod was  $\sim 12.5 \mu\text{m}$ , and for the plate,  $\lambda_2$  was  $\sim 3 \mu\text{m}$ . Therefore, the cooling rates were on the order of 150 K/s and  $1 \times 10^4 \text{ K/s}$ , respectively, for the rod and plate.

In order to change the processing parameters in DLF processing, an empirical balance between the powder flow rate, laser speed, and laser power must be made. In other words, if the laser traversing speed is increased, the powder flow (and possibly the laser power) must also be increased to

maintain a stable growth. Therefore, the processing parameter window is small, and independent variations of variables does not always result in a stable part. A variety of runs with slightly different parameters were made on the two Fe-based alloys, and the secondary dendrite arm spacings were evaluated. Considering the qualitative variations in processing conditions, the cooling rates vary between 50-10<sup>3</sup> K/s for the rods and 10<sup>3</sup>-10<sup>5</sup> K/s for the plates. Systematic quantified variations in the variables are currently being attempted and coupled with computer simulations to fully and completely interpret the effects of processing variables on the solidification behavior.

**Growth Rates.** The solidification rate in the DLF processing of rods should scale with the z-direction growth of the one dimensional part. For example, laser speeds can vary between 1 to 50 mm/s. If the laser speed exceeds the stable solidification speed, then a stable rod will not be maintained. Likewise, if the growth of the rod exceeds the laser speed, the rod growth will not be stable. In fact, the most stable rods are grown when the balance of powder flow rate into the puddle, the laser power, and laser speed provide a rod growth velocity that scales linearly with the laser speed.

Similar to the growth of rods, the growth of plates should scale with the beam velocity to maintain the growth of a uniform wall. In fact, the solidification growth velocities may be geometrically related to the heat flux direction, as in laser surface re-melting experiments [7]. For example, in surface re-melting studies, the growth angle,  $\theta$ , of a cellular or eutectic microstructure with respect to laser direction (horizontal) can be used to deduce the solidification velocity,  $V$ , by the following relation

$$V = V_b \cos\theta \quad (6)$$

where  $V_b$  is the laser beam speed.

Powder of Al-33wt.%Cu was used to evaluate the growth velocity during DLF processing. Eutectic spacings are proportional to the solidification rate, or growth velocity, of a solid/liquid interface [3]. For example, in the Al-33wt.%Cu eutectic composition, experiments have established that the lamellar spacing,  $\lambda$ , is proportional to the growth velocity,  $V$ , by the equation

$$\lambda = CV^{-n} \quad (7)$$

where,  $C = 1.04 \times 10^{-5} \text{ cm}^{3/2}/\text{s}^{1/2}$  and  $n = 0.5$  [8]. In this manner the growth orientation relation to the beam velocity as well as the eutectic spacing can be used to interpret the solidification velocity. However, a continuous wave laser could not produce uniform product in rod or plate form. At lower laser powers, a partially sintered product developed, and at higher laser powers, an uncontrolled molten sample was produced. Similar problems/observations have been reported in the laser welding of Al-based alloys [9]. Alternatively, a pulsed laser produced uniform product, presumably because the intervals between laser pulses permitted cooling and solidification..

A DLF grown plate of Al-33wt.%Cu is shown in Figure 6. The beam pass velocity for the sample was 6 mm/s,

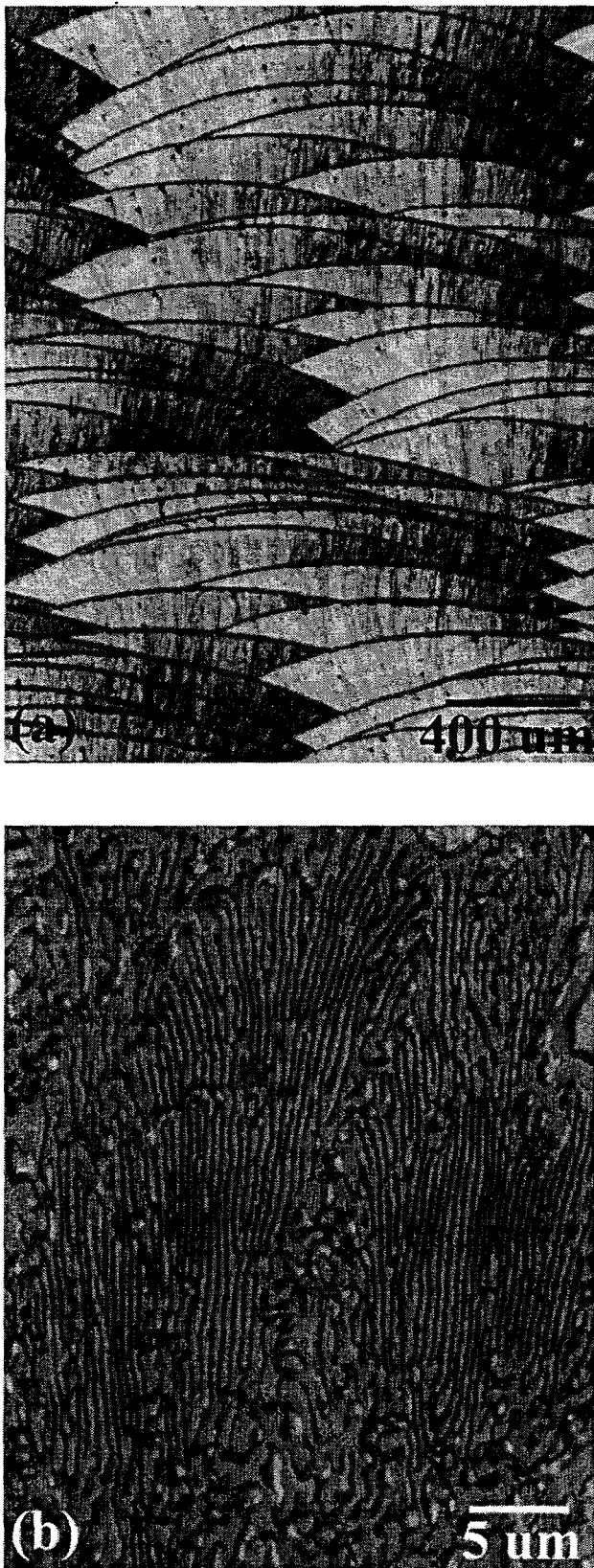


Figure 6 - (a) Low magnification and (b) high magnification optical micrographs of a Al-33wt.%Cu wall cross-section.

and Figure 6a demonstrates the possible effect of the pulsing (at 10 Hz) during processing. Discontinuous series (humps) of solidified product are evident in the fully dense product. At a velocity of 6 mm/s with 10 pulses/s, the hump spacing should be on the order of 600  $\mu$ m. In Fig. 6a, the hump spacing is 400  $\mu$ m to 800  $\mu$ m. Therefore, the wavy interface could, in fact, be attributed to the pulsing.

The growth orientation of the lamellar structure does not show distinct relation to the laser direction as was observed with the stainless steel in Figure 4. The eutectic spacing in this alloy (Fig. 6b) is approximately 300 nm, which through Eq. (7) yields a growth velocity of ~1.2 mm/s. Using Eq. (6), the angle of growth inclination should be 80°, and due to the "humped" structure, is difficult to ascertain. Nevertheless, the growth velocity is the same as growth velocities deduced in splat-quenching studies using the gun technique [8]. Although the growth orientation experiments did not yield the clearly discernable velocities, the eutectic spacing measurements illustrate that high growth velocities are attainable in the process

## Discussion

Since the DLF process is contained in a controlled environment and requires no preform, mold or crucible to contain the molten metal during processing, flexibility is possible in the types of materials (conventional, reactive, hazardous, or advanced materials). In fact, the DLF technique is more appropriately labeled as an advanced processing methodology which permits the novel processing of materials.

The advantage of the continuous solid/liquid interface region in the DLF process is that fully dense components can be produced. This contrasts to other near net shape liquid powder techniques (e.g. - thermal spraying) in that a molten droplet does not impact discontinuously onto a solid substrate, and as a result, structural integrity degradations attributed to splat gaps and other pore defects are absent. Therefore, optimized mechanical properties of as-cast structures can be produced.

Since continuous dendrite morphologies can be achieved through the continuous solid/liquid interface in DLF processing, the relatively high cooling and growth rates can be used to control and tailor microstructures, and therefore properties. Micro- and macrosegregation in cast components can lead to structural anomalies in terms of the physical properties of the materials. Studies have shown that reduced macrosegregation in cast components permits optimized strengths of the multi-phase materials, particularly steels [10]. In addition, owing to the small molten pool which is continuously fed with uniform composition of powder, macrosegregation is absent [1].

The refined microstructures in DLF processing are attributed to the controlled molten pool during processing and the high cooling and growth rates during solidification.

The two dimensional plates exhibit higher cooling rates than the one dimensional rods. For the plates, the prior substrate experiences a period of time for cooling before deposition occurs again. The cooler substrate provides a larger driving force for conduction cooling as compared to the rod, where the heat flux by conduction cooling is constant down the growth direction.

As a result of defining the solidification behavior in DLF processing combined with the fully dense components, more diverse, novel, or advanced materials can be processed. For example, bulk intermetallic geometries can be produced for testing of properties without cumbersome fabrication or machining steps. In addition, controlled solidification science studies are capable with growth and cooling rates that are higher than in, for example, conventional directional solidification studies. Furthermore, bulk rapid solidification product (cooling rates  $> 10^4$  K/s) can be produced without consolidation techniques to evaluate the bulk properties. All of these efforts are currently in progress.

## Conclusions

A variety of metals have been processed with directed light fabrication, and the laser fusing of metal powders results in three main features during solidification:

- (1) a continuous solid/liquid interface
- (2) average cooling rates on the order of  $10^2$  K/s for rods and  $10^4$  K/s for plates, and
- (3) growth rates that can vary from 1 to 50 mm/s.

As a result, the novel processing of most any metal (high-temperature, reactive, or hazardous) can be fabricated while maintaining fully dense product and uniformly refined microstructural features.

## Acknowledgments

The authors wish to thank Ann M. Kelly of Los Alamos National Laboratory (LANL) for metallographic preparations and Dr. Loren A. Jacobson and John O. Milewski (LANL) for comments on the manuscript.

## References

- 1 Lewis, G.K., R.B. Nemec, J.O. Milewski, D.J. Thoma, M. Barbe, and D. Cremers, Proc. ICALEO (LIA, Orlando, FL) p. 17 (1994).
- 2 Burns, M. "Automated Fabrication: Improving Productivity in Manufacturing", pp, PTR Prentice Hall, Englewood Cliffs, NJ, (1993).
- 3 Kurz, W. and D.J. Fisher, "Fundamentals of Solidification", 3rd ed., Trans Tech Publications, VT, (1989).
- 4 Brower, Jr., W.E., R. Strachan, and M.C. Flemings, AFS Cast Metals Research Journal, Dec., p. 176, (1970).
- 5 Katayama, S. and A. Matsunawa, Proc. ICALEO, p. 60 (1984).
- 6 Elmer, J.W., S.M. Allen, and T.W. Eagar, Metall. Trans. A, 20A, p. 2117, (1989).
- 7 Carrupt, B., M. Rappaz and M. Zimmerman, "Modeling of Casting and Welding Processes IV", A.F. Giamei and G.J. Abbaschian, eds., p. 581, TMS, Warrendale, PA, (1988).
- 8 Burden, M.H. and H. Jones, J. of the Inst. of Metals, vol. 98, p. 249, (1970).
- 9 ????? laser welding of Aluminum
- 10 Kattamis, T.Z. and R. Mehrabian, J. Vac. Sci. Technol. vol. 11 #6, p. 1118, (1974).